Low Energy Electron Spectrometer Construction

Y. Glinec, J. Faure, A. Guemnie-Tafo, V. Malka

Laboratoire d'Optique Appliquée –ENSTA, UMR7639, CNRS, Ecole Polytechnique, 91761 Palaiseau, France

H. Monard, J.P. Larbre, V. De Waele, J.L. Marignier, M. Mostafavi

Laboratoire de Chimie Physique / ELYSE, Université Paris Sud 11, 91405 Orsay, France

Acknowledgements

We acknowledge the support of the European Community-Research Infrastructure Activity under the FP6 "Structuring the European Research Area" programme (CARE, contract number RII3-CT-2003-506395)

Low Energy Electron Spectrometer Construction

Y. Glinec, J. Faure, A. Guemnie-Tafo, V. Malka

Laboratoire d’Optique Appliquée – ENSTA, UMR7639, CNRS, Ecole Polytechnique, 91761 Palaiseau, France

H. Monard, J.P. Larbre, V. De Waele, J.L. Marignier, M. Mostafavi

Laboratoire de Chimie Physique / ELYSE, Université Paris Sud 11, 91405 Orsay, France

This work was supported by the European Community Research Infrastructure Activity under the FP6 “Structuring the European Research Area” program (CARE, contract number RII3-CT-2003-506395).

Low energy electron spectrometer prototype

The spectrometer prototype is composed by :

- A magnet : to deflect electrons
- A scintillator : Phosphor layer to convert electrons into light
- Optics to transport light to the detector
- CCD Camera to record the image of the scintillator on a computer

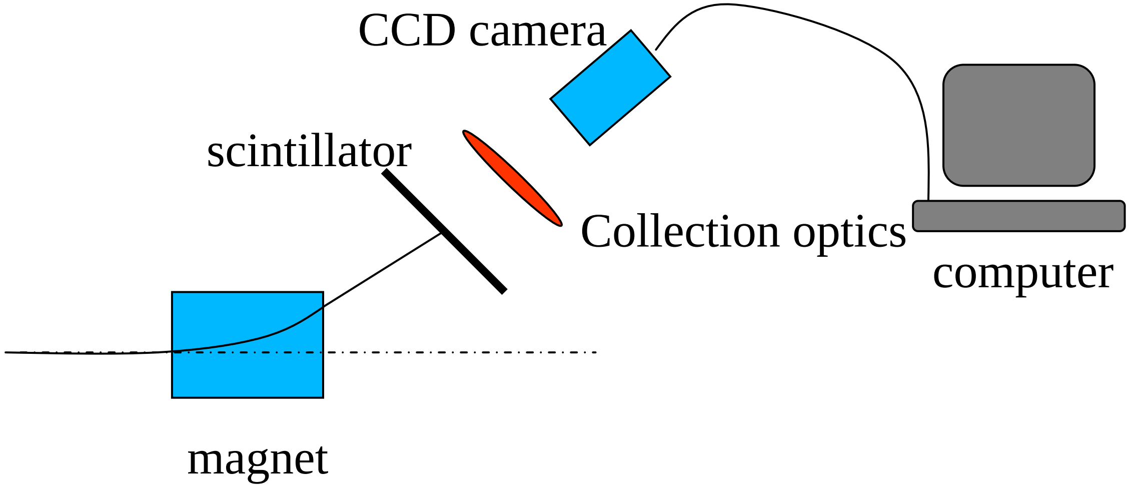

Scheme of principle of the prototype

1) The Magnet

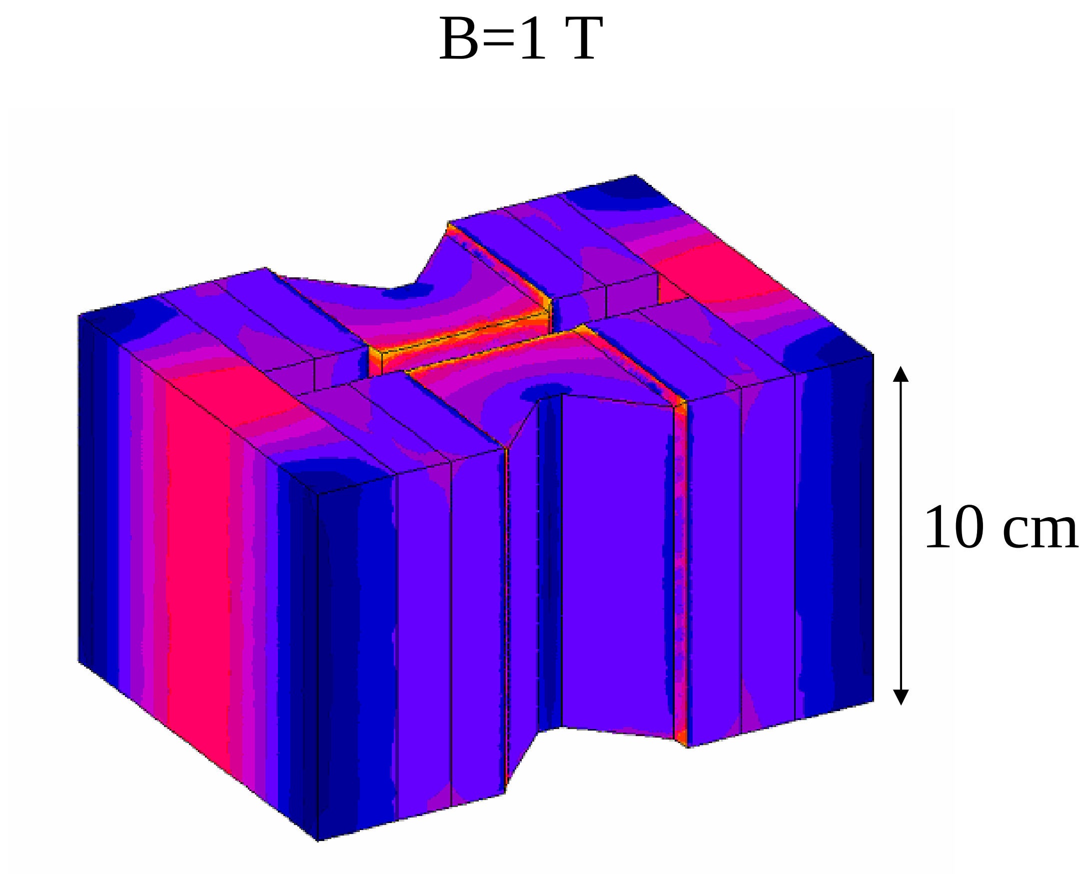

Design of a new magnet up to 200 MeV

Higher electron energy can be measured (up 400 MeV but with low spectral resolution)

Datasheet

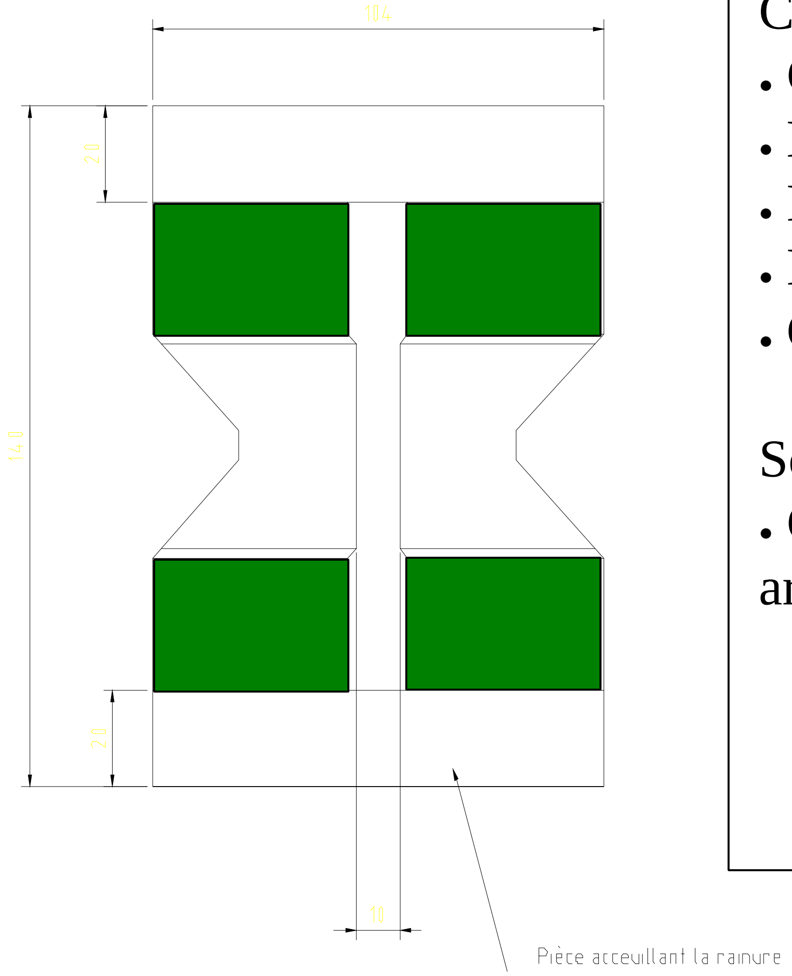

Constraints :
- Gap = 1cm
- Magnetic field ~ 1T
- Length = 10 cm
- Large slit required
- Compact spectrometer

Solution :
- Good homogeneity due to a special arrangement of magnet poles

Data from the manufacturer

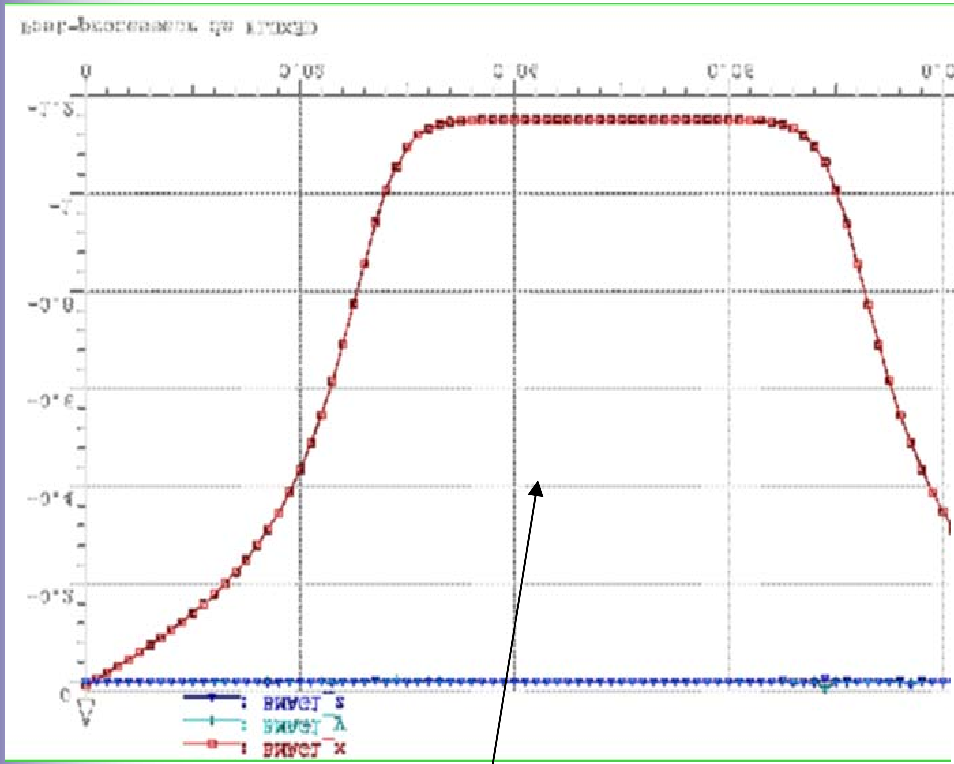

Simulations of the longitudinal magnetic field

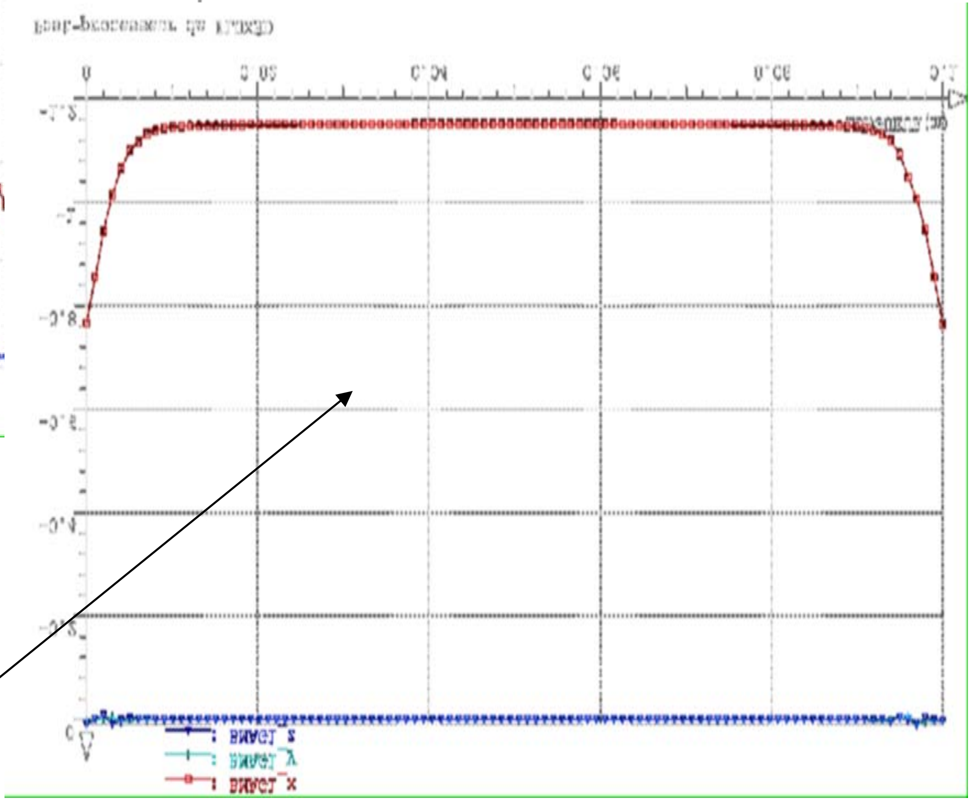

Transverse magnetic field

Analytical calculations

- Trajectories of an electron in a permanent magnetic field
  - Radius of curvature (relativistic electron):

$$R = \frac{E_0}{B_m e c}$$

E_0 Initial kinetic energy
B_m Magnetic field
e Charge of the electron
c Celerity of light

- Assumptions :
  - The magnetic field is uniform in a rectangular area
  - The relativistic incomming electron is perpendicular to the magnet's surface.

Coordinates

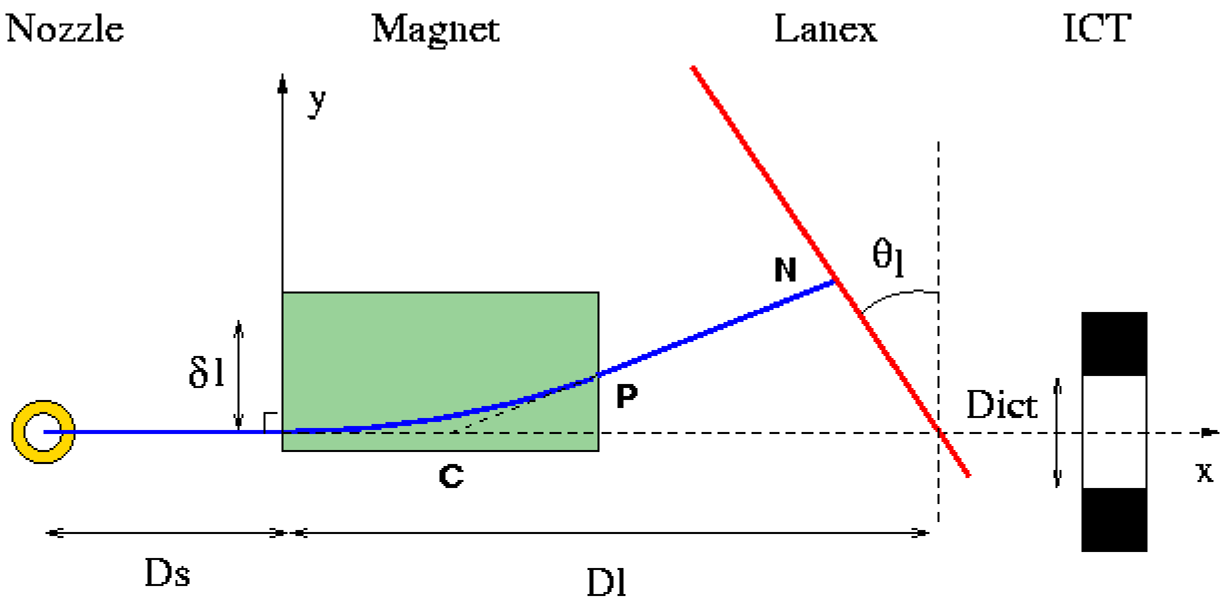

$$\begin{pmatrix} x_P \\ y_P \end{pmatrix} = \begin{pmatrix} L_m \\ R-\sqrt{R^2-L_m^2} \end{pmatrix} \qquad \begin{pmatrix} x_C \\ y_C \end{pmatrix} = \begin{pmatrix} \dfrac{x_P^2+y_P^2}{2\,x_P} \\ 0 \end{pmatrix} \qquad \begin{pmatrix} x_N \\ y_N \end{pmatrix} = \begin{pmatrix} D_l - y_l \tan(\theta_l) \\ \dfrac{(D_l - x_C)\,y_P}{x_P - x_C + y_P \tan(\theta_l)} \end{pmatrix}$$

Equivalent magnetic field

- The real magnetic field spreads outside the magnet. The introduction of an equivalent magnetic field allows the use of analytical formulas.

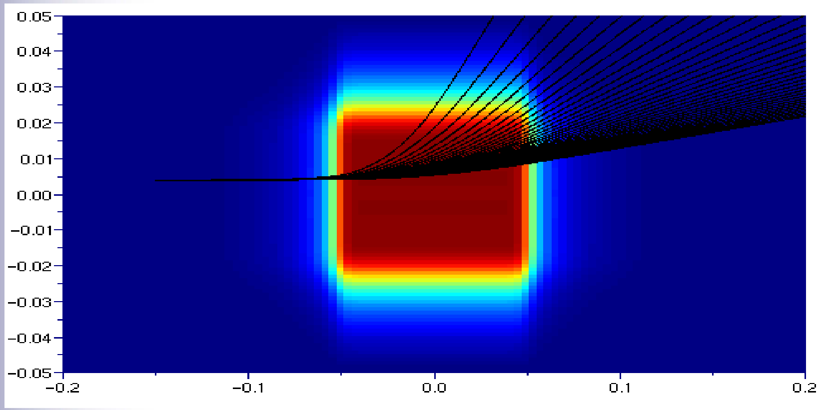

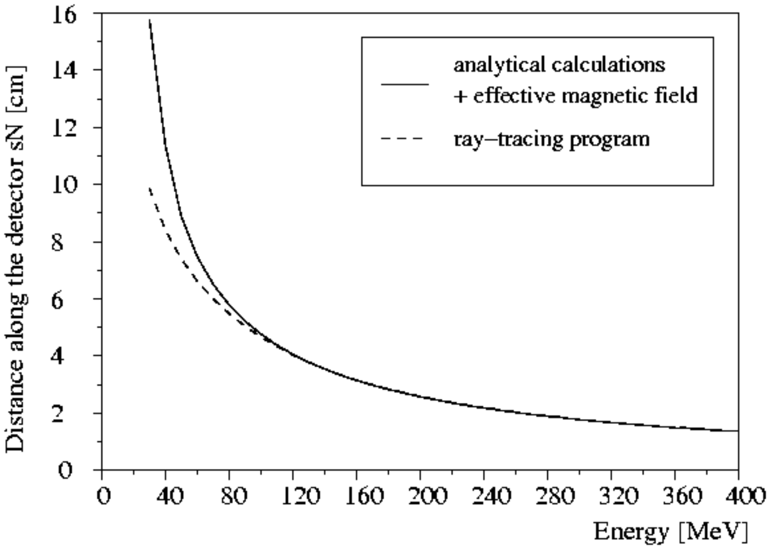

$$B_m^{max} = 1.0\,T \longrightarrow B_m^{eff} = 1.29\,T$$

- Not valid for electrons below 100 MeV who travel in the gradient of the magnetic field

Resolution

- The resolution is limited by the size of the electron beam on the detector. The corresponding energy range at a given energy E_0 is :

$$\frac{\delta E_0}{E_0} = \frac{\delta_s}{E_0} \div \frac{ds_N}{dE_0}$$

$s_N = y_N/\cos(\theta_l)$ the distance along the Lanex

δ_s the size of the electron beam on the detector

- The equivalent at high energy is

$$\frac{\delta E_0}{E_0} \sim \frac{(D_s + D_l) R \theta_s}{(D_l - L_m/2) L_m} \propto R \propto E_0$$

θ_s divergence

Energy [MeV]	20	50	100	200	400
Prototype	-	-	5%	10%	20%

Resolution for two different configurations

Picture of the Magnet Prototype

(used in the experiment in two experiments)

2) The Scintillator : Detector composition

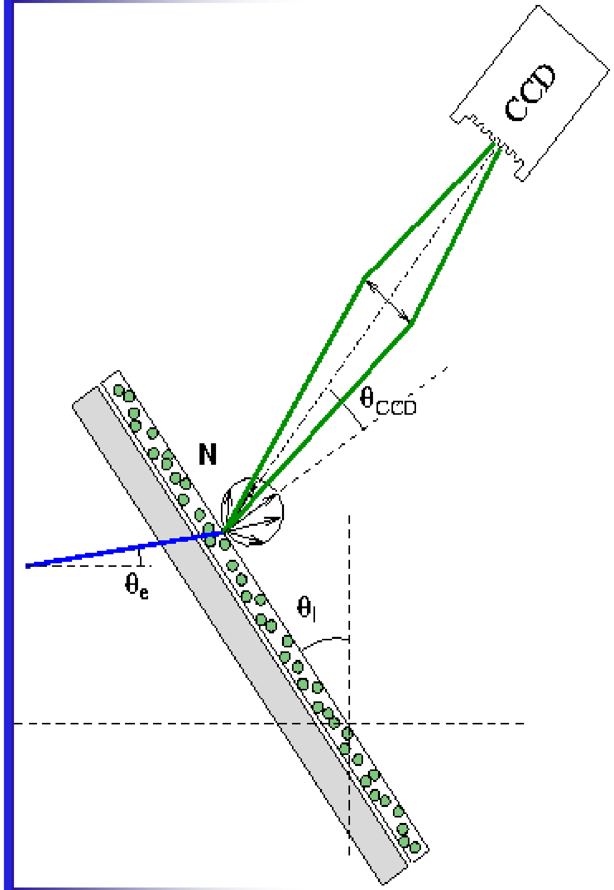

Item	*Material*	*Density (g/cc)*	*Thickness (cm)*
Laser Shielding			
Shielding	Aluminium	2,70	0,0100
Kodak Lanex Fine Screen			
protective coating	cellulose acetate	1,32	0,0010
plastic subtrate	Poly(ethylene terephtalate)	1,38	0,0178
scintillator	Gd2O2S + urethane binder	4,25	0,0084
protective coating	cellulose acetate	1,32	0,0005

Composition of the scintillating screen

The surface loading of Gadolinium Oxysulfide in the urethane binder is 33 mg/cm^2

Schach von Wittenau *et al.*, Med. Phys. **29** pp. 2559-2570 (2002)

3) Absolute calibration

Phosphor layer : conversion

We assume that the conversion into visible light is proportional to the energy deposited in the scintillator layer

$$\frac{dN_{cr}}{dN_{el}} = \frac{1}{E_{ph}} \varepsilon \frac{dE}{dx} \delta x$$

$\delta x = h_S / \rho_{GOS}$ effective phosphor thickness

ε efficiency

Transport : photon collection

The transmission at the phosphor boundary and the number of photons collected by the lens of the Andor CCD

$$\frac{dN_{coll}}{dN_{cr}} = \zeta \, g(\theta_{CCD}) \, \delta\Omega \, q_I q_Q q_{IF}$$

ζ output transmission factor

$g(\theta_{CCD})$ lambertian law

Detection by the CCD : number of counts

The yield of the Andor CCD camera

$$\frac{dN_{count}}{dN_{coll}} = \frac{QE}{r}$$

$$\frac{dN_{el}}{dE} dE = Counts \div \left(\frac{dN_{counts}}{dN_{coll}} \frac{dN_{coll}}{dN_{cr}} \frac{dN_{cr}}{dN_{el}} \right)$$

List of parameters

Parameter	Symbol	Value
Spectrometer		
Magnet		
Equivalent magnetic field	Bm	0.41 T
Magnet length	Lm	5 cm
Magnet width	Lm	2.5 cm
Magnet shift	δlm	1.3 cm
Magnet-Lanex length	Dl	17 cm
Lanex		
Lanex angle	θl	55°
Efficiency	ε	0.16
Surface Loading	hs	33 mg/cm2
Phosphor density	ρ_{GOS}	7.44 g/cm3
Photon energy	Eph	2.27 eV
Transmission factor	ζ	0,22
ICT		
ICT diameter	Dict	10 cm

Parameter	Symbol	Value
Detection System		
Solid Angle	δΩ	2.0e-3 sr
CCD angle	θccd	15°
Lens	q_l	0,95
Quartz	q_q	0,95
Interference filter	q_{IF}	0,2
Pixel size on the lanex	L_{pix}	0.28 mm
Electron Source		
Source-Magnet length	Ds	6 cm
Divergence	θs	10 mrad

From absolute calibration at ELYSE

The absolute calibration of the LANEX KODAK FINE

In collaboration with ELYSE

- Calibration of the scintillator response on a RF accelerator
  - ELYSE : a laser-triggered picosecond electron accelerator

Linearity with charge

Independence of the yield with electron energy

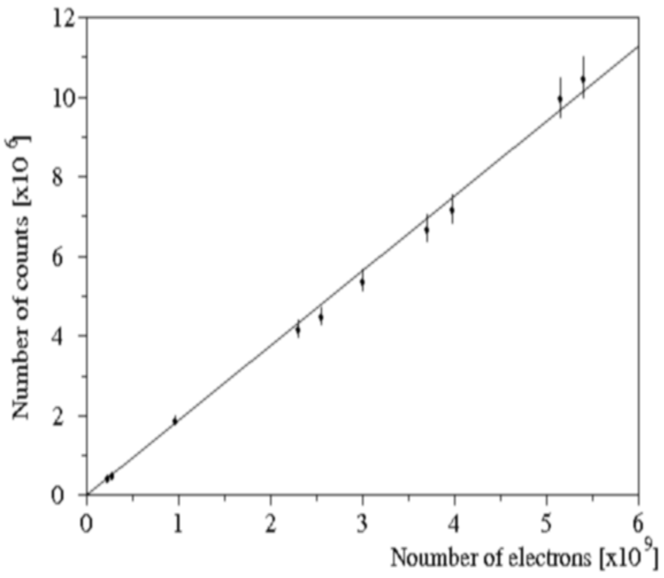

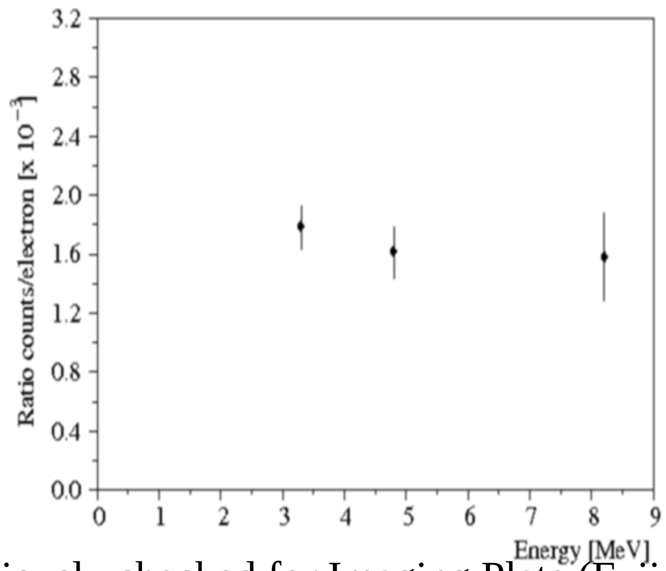

Previously checked for Imaging Plate (Fuji BAS-SR2025) : Tanaka *et al*., Rev. Sci. Instr. (2005)

Extension for laser-plasma interaction

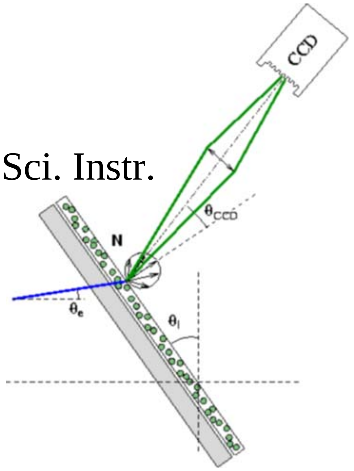

- Global yield of the detection system
  - Intrinsic yield of pure GOS : independent of the electron energy (Tanaka *et al*, Rev. Sci. Instr. 2005)
  - Transmission factor at the interface and output light distribution
  - Collection angle of the lens and conversion into number of counts on the CCD chip.

- Assumption that the scintillator efficiency remains constant
  - Retrieve the intrinsic conversion efficiency of this scintillator (fraction of energy deposited in pure GOS layer which is converted into visible light)

♏ ~ 16 %

  - Surprisingly close to the value for X-rays (in the range 15-20 %) : Giakoumakis *et al*, Phys. Med. Biol. (1989)
  - Can be used in other configurations

Glinec *et al*, accepted in RSI

Prototype tests : Experimental setup

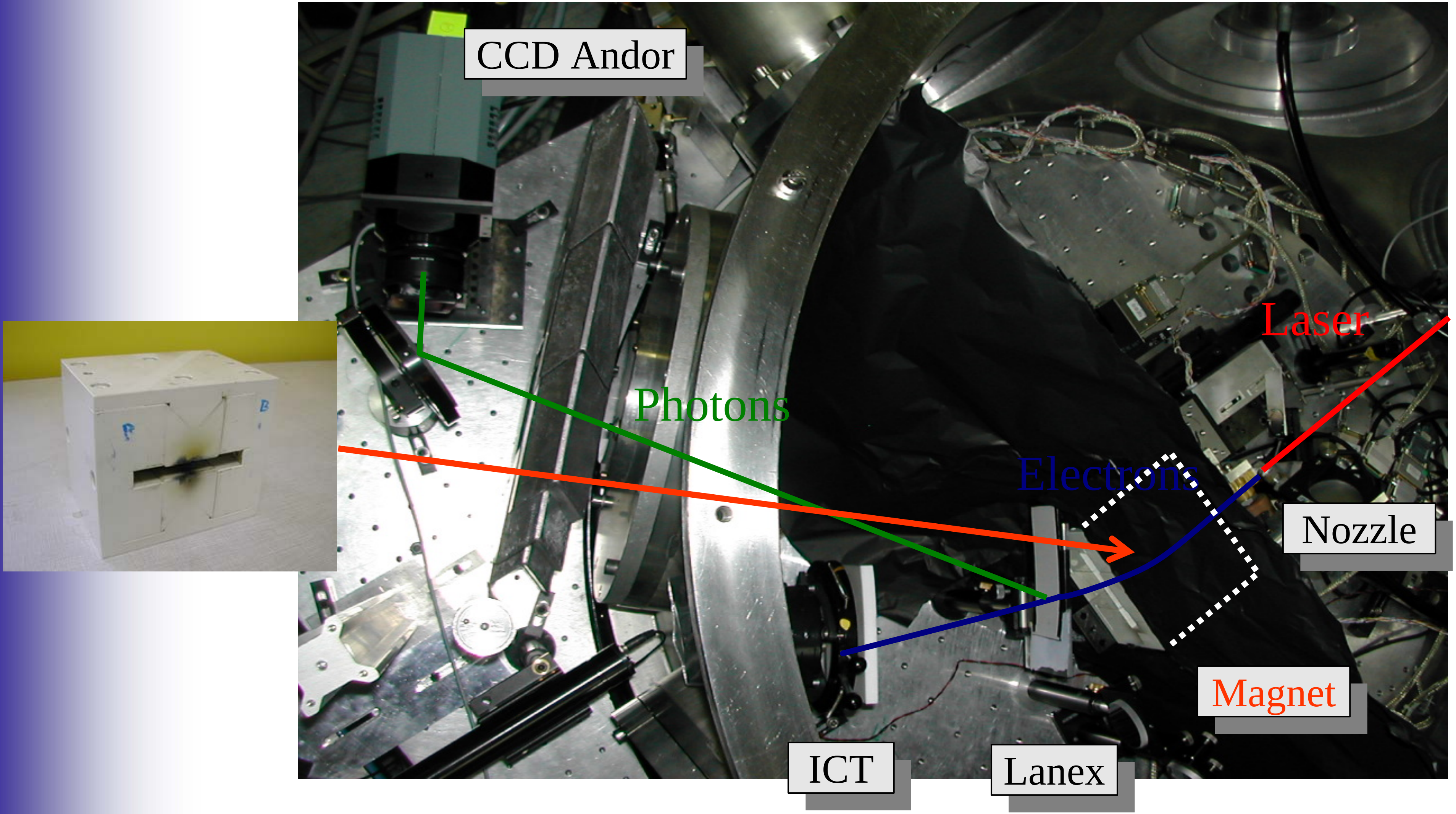

The back cloth is used to reduce the laser and visible light in the camera
A picture of the magnet is also shown on the following slide

Prototype test

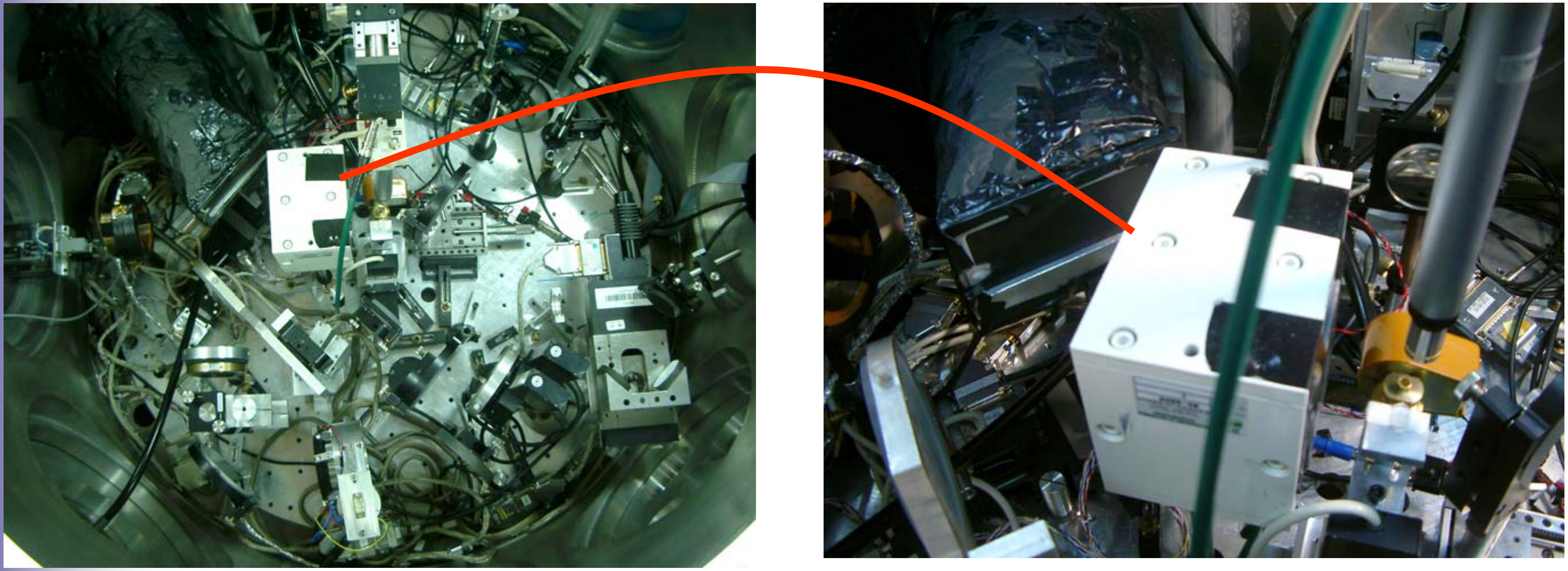

Vacuum chamber

Magnet

Test n°1 of the prototype

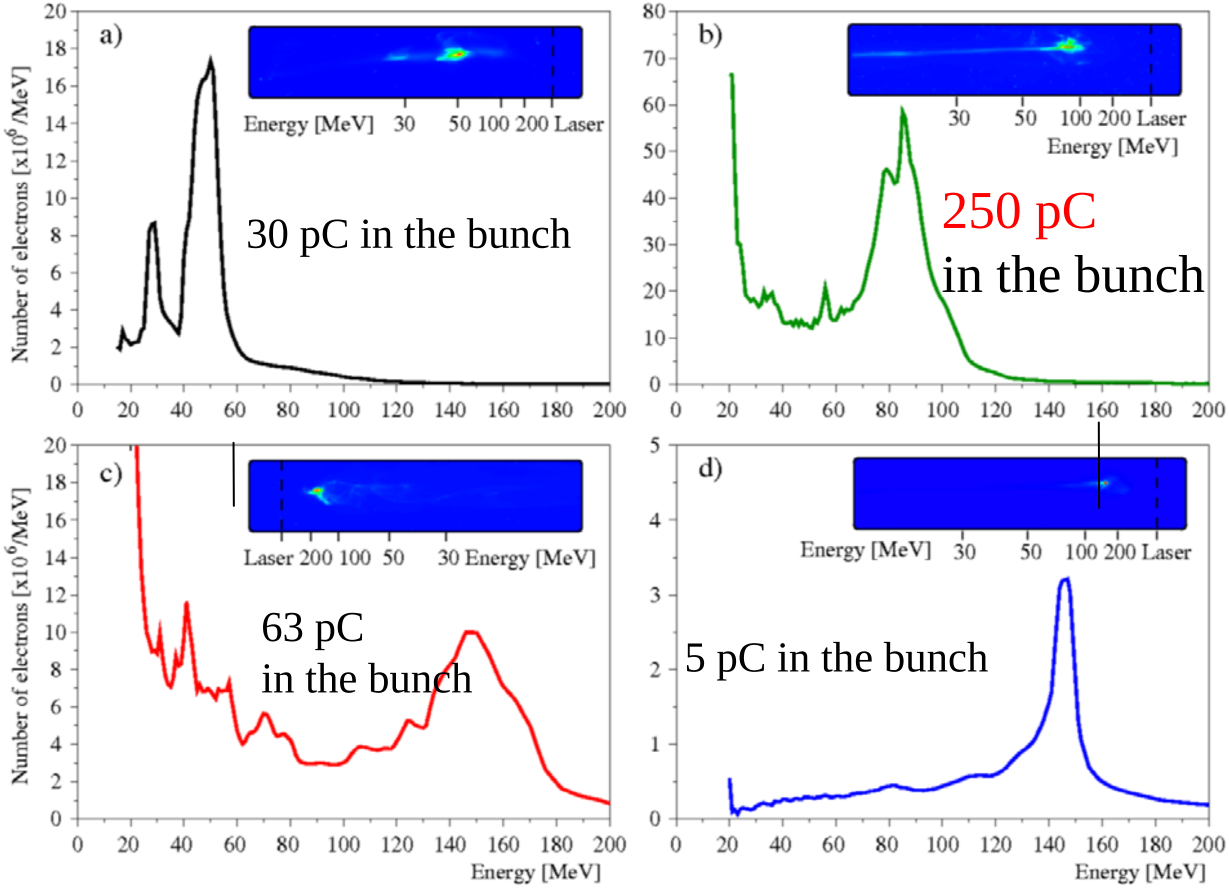

30 pC in the bunch

250 pC
in the bunch

63 pC
in the bunch

5 pC in the bunch

dE/E ~ 6%

Electron beam distribution obtained with the prototype

Conclusion and Perspectives

I – Needs for a compact single shot spectrometer

- Requirements
  - Acceleration of electrons up to 200 MeV.
  - Adapted to high repetition rate : no film processing.
- Solution chosen
  - Design and purchase of a strong permanent magnet
  - Purchase of 16 bits Andor CCD cameras.
  - Development of analytical formulaes for spectrum deconvolution
  - Purchase of a hall probe for magnet characterization
- Estimation of the efficiency of the scintillator, absolute calibration

II – Further developments

- The present work will help the design of a larger magnet for GeV acceleration experiments